# HEAT TRANSFER PERFORMANCE OF AN OIL JET IMPINGING ON A DOWNWARD-FACING STAINLESS STEEL PLATE

by

***Roy J. ISSA***

Department of Engineering and Computer Science,
Mechanical Engineering Division, West Texas A&M University, Canyon, TX., USA

Original scientific paper
UDC: 621.78.08:621.892.6:536.22
DOI: 10.2298/TSCI090406011I

*An experimental study is carried out for the quenching of a stainless steel plate using a single oil jet impinging on the bottom surface of the plate. The objective of this study is to investigate the effect of the oil jet flow operating conditions on the heat transfer effectiveness when the plate is heated to temperatures ranging from around 115 to 630 °C, and the oil is heated to temperatures ranging from 60 to 75 °C. Tests are conducted on the oil at various temperatures to determine its viscosity. Experiments are conducted for nozzle exit flow rates ranging from 113 to 381 ml/min., oil jet pressures from 3.1 to 12 psi, and nozzle-to-plate surface distances of 0.6 and 1 cm. The variation of the oil heat flux and heat transfer coefficient with the surface temperature for the different quenching parameters is calculated from the acquired temperature data. Tests results show the oil heat transfer effectiveness keeps increasing for increasing plate temperature. Oil jet pressure is shown to have a considerable effect on the oil heat transfer, while the nozzle-to-plate surface distance is shown to have a lesser effect. The results of this study shall lead to a better understanding of the parameters that play an important role in oil quenching for applications that are of interest to the metal process industry.*

Key words: *oil jet, oil pressure, heat flux, heat transfer*

## Introduction

Quenching of steel material has been the subject of investigations and experience with different cooling systems for many years. Cooling by forced air has very low heat transfer effectiveness. At room temperature, forced air convection has a maximum heat flux ranging from 0.02 to 0.03 kW/m$^2$. Water has much superior thermo-physical properties. Quenching by water bath (pool boiling) can provide heat fluxes that range from 20 to 1,500 kW/m$^2$ [1]. Water jets provide much higher cooling rate (~6,000 kW/m$^2$) [2-4]. Multi-phase cooling using air-assisted water sprays can generate cooling heat fluxes between 1000 to 10,000 kW/m$^2$ at atmospheric pressure conditions depending on the liquid mass flux [5, 6]. Oil has lower thermo-physical properties than that of water, and as a quenchant it is expected to provide heat fluxes lower than that for water pool boiling. However, little is known in the

* Author's e-mail: rissa@mail.wtamu.edu

open literature about the quenching process of a steel plate bottom surface when oil is used as a quenchant.

Quenching of steel material by water jets or sprays is corrosive to the ferrite material because of the oxidation layer that quickly builds up on the steel surface. Therefore, water has detrimental effect on the steel surface quality. Quenching by oil has been commercially used in industrial applications where surface quality is of concern and achieving high cooling rates is not an issue. Several investigators have studied the heat transfer associated with immersion in an oil bath. Chen *et al*. [7] conducted tests on oil quenching of machined connecting rods for high-power diesel engine. Oil was shown to have lower cooling power compared to other quenchants such as water and aqueous polymers. Abou-Ziyan [8] investigated the pool boiling heat transfer from high temperature parts in internal combustion engines. Oil was heated at atmospheric pressure to temperatures ranging from 40 to 175 °C, and the cast iron test specimen was heated to 200 °C above the oil saturation temperature. Lower oil temperatures resulted in higher heat transfer capability. Prabhu *et al.* [9], and Fernandes *et al.* [10], conducted pool quenching experiments on AISI 304 stainless steel and AISI 1040 steel specimens immersed in palm oil and mineral oil baths. Palm oil was shown to have slightly higher cooling power than mineral oil in still pool. Agitation of the pool was shown to improve the heat transfer capability. De Paepe *et al*. [11] investigated the performance of oil cooling by atomization in an oil injected screw compressor. Their experiments showed that reducing the oil droplet size considerably enhanced the heat transfer. Ma *et al*. [12] investigated the local convective heat transfer from a vertical heated surface to an obliquely impinging free-surface jet of transformer oil. The heat transfer coefficient was found to decrease with the increase in jet inclination. Akbarpour [13] conducted mechanical property tests on triple phase steel plates where oil was used to pool quench the steel from 400 °C to room temperature after the plates were annealed at 780 °C and held isothermally for several minutes at 400 °C. Tensile tests showed the yield and ultimate tensile strength decreased with increasing temperature. Zhukauskas *et al.* [14] conducted experiments on the quenching of 50 mm and 100 mm wide plates immersed in a rectangular channels 100 × 50 mm and 100 × 200 mm in cross-section, respectively. Turbulent flow conditions were created and varieties of fluids were used including transformer oil.

Although there have been some studies published on oil quenching, most of these studies have been performed on the immersion of test specimens in an oil bath (pool boiling). Very limited studies have been conducted on oil using jets impinging downward on a surface. Furthermore, there is also lack of studies conducted on upward jet impingement using oil. Several factors will influence the cooling effectiveness of an oil jet that is impinging upward on a heated surface. Some of these factors include: oil pressure and flow rate, nozzle-to-plate distance, and plate temperature.

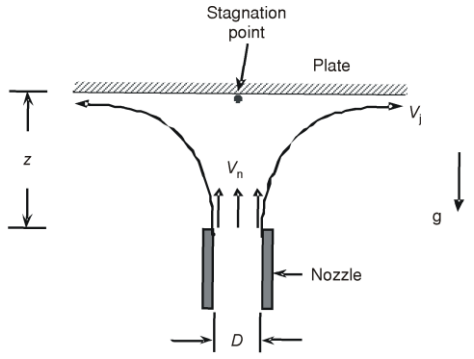


**Figure 1. Schematic of the oil jet configuration**

Figure 1 represents the condition for a planar, free-surface oil jet impinging on the bottom surface of a plate. The flow velocity is zero at the stagnation point but increases to the jet surface velocity with the increasing distance along the surface. On the other hand, the pressure is a maxi-

mum at the stagnation point due to the dynamic contribution of the impinging flow, but decreases to the ambient pressure with the increasing distance along the surface.

For an upward jet impingement, the velocity of the free-surface jet varies between the nozzle exit velocity, $V_n$, and the jet surface velocity, $V_s$. Gravity decelerates the free-surface jet velocity with the increase in the vertical distance according to the following relationship:

$$V_s = \sqrt{V_n^2 - 2gz} \tag{1}$$

Oil jets having low incoming momentum result in poor cooling because the oil film can not spread effectively on the surface. The more the oil film spreads during impaction, the higher will be the cooling effectiveness. For a downward-facing surface, oil flooding on the surface is not an issue to be concerned with, and this acts favorably on the heat transfer. However, for the same flow operating conditions as that for a top surface, the jet impactions on a downward-facing surface is weaker than that on an upward facing surface due to the effect of gravitational and drag forces acting on the jet. Therefore, a higher oil jet pressure (or higher oil mass flow flux) is needed to increase the impaction force on the bottom surface.

## Experimental set-up

Figure 2 shows the overall experimental system set-up. The oil used in the conducted tests is SAE 5W-30 synthetic oil having a flash point temperature higher than that of non-synthetic oil. A digital gear-pump by Fisher Scientific Inc. increases the oil pressure to a level necessary for jet injection. The gear pump provides a continuous oil flow rate that ranges from about 113 to 381 ml/min. for the current experimental setup. Oil is heated to a temperature ranging from 60 to 75 °C before it is pumped. This temperature range sufficiently lowers the oil viscosity to ensure smooth and continuous flow for the oil jet exiting the nozzle. The heating of the oil is achieved by placing the oil reservoir into a hot water bath. The water temperature is controlled by two electric resisters and the oil temperature is closely monitored. An oil chamber is built to retain the oil after it makes impact with the plate, fig. 3(a). Drainage from the base of the oil chamber directs the flow back to the oil reservoir. A flow rate and a pressure gauge are installed on the PVC tube leading to the nozzle manifold. The nozzle manifold system is custom made using stainless steel material, and has an exit orifice diameter of 1 mm.

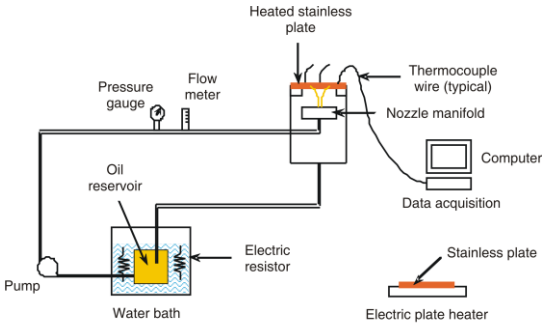


**Figure 2. Overall experimental system set-up**

The test section consists of a square stainless steel plate with a side dimension of 7 cm, and a thickness of 4.2 mm. Fifteen holes (2 mm in diameter, and 2 mm deep) are drilled from the top side of the plate. Figure 3(a) shows a close-up view of the location of the drilled holes along the plate. Nine thermocouples of type K are imbedded inside the drilled holes to record the temperature variation during the quenching of the plate. A plate heater from Omega Engineering is used to heat the plate to temperature ranging from 115 to 630 °C. Once the

**Figure 3(a). Oil jet chamber**

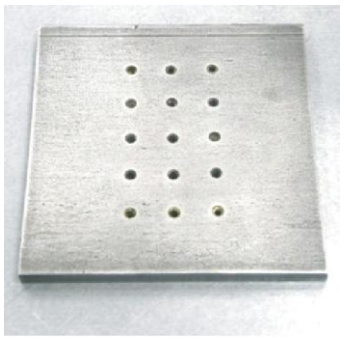

**Figure 3(b). Stainless steel plate**

plate reaches the desired temperature, it is removed and positioned on a holding rack above the nozzle manifold – refer to fig. 3(b), that has a nozzle exit of 1 mm in diameter. In this study, the dimensions of the steel plate are selected to be large compared to the oil jet diameter. This is because the objective of this research is to study the heat transfer for a mild oil quenching process. An additional thermocouple is cemented on the cartridge heater surface to control the temperature setting of the heater. Two more thermocouples are also used to record the ambient and oil temperatures. All thermocouple wires are connected to a data acquisition device (Omega OMB-CHARTSCAN-1400), which in turn is connected to a portable computer that records the temperature data on the hard disk drive at a rate of 1 data point per second. To reduce any signal noise during sampling, the data acquisition device was set to average every 32 measurements per line cycle per channel. In the tests conducted during this study, the quenching of the steel plate by oil did not produce very rapid initial heat transfer. This is because the oil flow rate that was selected in the tests was relatively low. In addition, oil does not have a high cooling power compared to other fluids such as water. Therefore, the data recording rate and the data averaging technique that was adopted was deemed appropriate for the conducted tests. Table 1 shows the uncertainties in the experimental data.

**Table 1. Uncertainties in experimental data**

| Variables | Uncertainty |
|---|---|
| *Measured variables* | |
| – Temperatures (K-type thermocouples) | ±1.1 °C |
| – Oil pressure | ±3% |
| – Oil flow rate | ±4% |
| – Dimensions | ±0.05 mm |
| – Properties | Negligible |
| *Calculated variables* | |
| – Oil heat transfer coefficient | ±11% |

## Results and discussion

### *Oil viscosity tests*

Rheology tests were conducted on the synthetic oil using a digital Brookfield viscometer (Model No. LVDV-II+Pro) to determine the constitutive equations of the fluid at various operating temperatures: 23.5 (room temperature), 50.1, and 67.0 °C. Brookfield viscometer measures the torque required to rotate a spindle of known dimensions while being immersed in the test fluid. In this study, LV-1 type of spindle is used. (This is a cylindrical spindle with the following dimensions: spindle length: 6.51 cm, and spindle diameter: 1.884 cm). The maximum spring torque provided by the motor is $67.3 \cdot 10^{-6}$ Nm.

The constitutive equation for a non-Newtonian fluid can be represented by the power law or Ostwald-de-Wale equation given by:

$$\tau = K\dot{\gamma}^n \tag{2}$$

where $K$ is a consistency coefficient and $n$ is the power law index of the flow. $n$ can be experimentally calculated from the slope of the double logarithmic plot for the motor torque *vs.* spindle angular velocity [15]:

$$n = \frac{\mathrm{d}\ln T_\mathrm{m}}{\mathrm{d}\ln \omega} \tag{3}$$

Figure 4 shows the viscometer motor torque *vs.* the spindle angular velocity. The calculated power law index is shown to range from 0.99 to 1.04 for the three oil temperatures that are tested. Since $n$ is close to 1, this suggests that the synthetic oil is behaving like a Newtonian fluid at all temperatures.

In a Brookfield viscometer, the spindle is driven by a motor through a calibrated spring. The shear stress at the spindle is proportional to the motor torque and is calculated as:

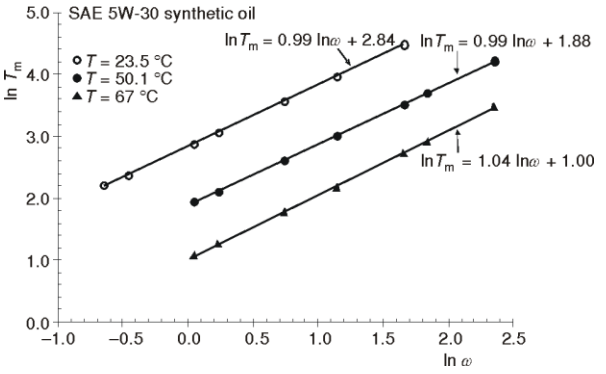


**Figure 4. Motor torque *vs.* angular velocity (full synthetic motor oil)**

$$\tau = \frac{T_\mathrm{m}}{2\pi R_\mathrm{s}^2 L} \tag{4}$$

The shear rate for this Newtonian fluid can be evaluated at the spindle wall and is shown to be proportional to the spindle angular velocity:

$$\dot{\gamma} = \frac{2\omega R_\mathrm{c}^2}{R_\mathrm{c}^2 - R_\mathrm{s}^2} \tag{5}$$

The radius for the oil container, $R_\mathrm{c}$, is 4.175 cm. Because the tested oil behaves in a Newtonian fashion, its constitutive equation can then simply be expressed by:

$$\tau = \mu\dot{\gamma} \tag{6}$$

where $\mu$ is the oil dynamic viscosity. The effect of temperature on the oil's dynamic viscosity is very strong (as shown in fig. 5). The dynamic viscosity is calculated from the slope of the linear curve relating the shear stress to shear rate. The viscosity is shown to drop considerably from 0.015 Ns/m$^2$ at 23.5 °C to 0.0027 Ns/m$^2$ at 67 °C, a decrease of more than 80% in viscosity for a temperature increase of 43.5 °C. For this temperature range, a correlation between the viscosity and operating temperature can then be obtained:

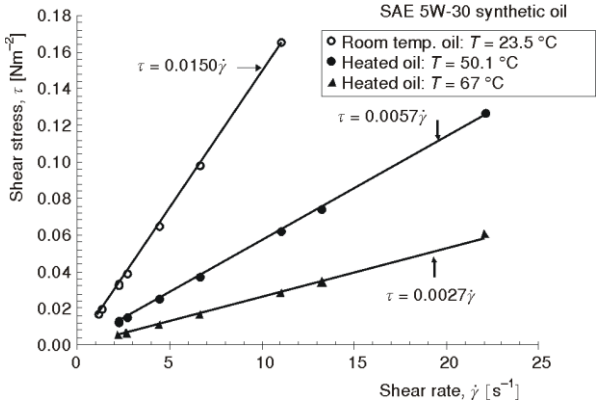


**Figure 5. Shear stress *vs.* shear rate for oil**

$$\mu = 3.96 \cdot 10^{-6} T^2 - 6.41 \cdot 10^{-4} T + 2.79 \cdot 10^{-2} \quad (7)$$

### *Heat transfer test measurements*

As mentioned earlier, there are several factors that influence the heat transfer effectiveness during oil quenching. These include oil temperature, oil pressure, target surface temperature, and nozzle-to-surface distance. Simulation results will be presented to portray the sensitivity effect of these parameters. Table 2 shows the conducted test cases.

**Table 2. Test cases operating conditions**

| Case No. | $T_i$ [°C] | $T_{oil}$ [°C] | $T_{air}$ [°C] | $P_{oil}$ (psi) | Oil flow rate, $Q$ [ml/min.] | Jet distance, $z$ [cm] |
|---|---|---|---|---|---|---|
| 1 | 115 | 64.8 | 27.8 | 3.2 | 117 | 1 |
| 2 | 144 | 58.8 | 23.4 | 3.2 | 117 | 1 |
| 3 | 202 | 58.7 | 24.9 | 3.3 | 121 | 1 |
| 4 | 284 | 58.5 | 24.8 | 3.1 | 113 | 1 |
| 5 | 417 | 65.0 | 28.0 | 3.4 | 125 | 1 |
| 6 | 535 | 75.2 | 27.2 | 3.4 | 125 | 1 |
| 7 | 615 | 65.0 | 28.5 | 3.1 | 113 | 1 |
| 8 | 124 | 61.5 | 27.0 | 5.8 | 210 | 1 |
| 9 | 238 | 63.5 | 27.9 | 5.6 | 205 | 1 |
| 10 | 314 | 66.3 | 28.3 | 5.6 | 205 | 1 |
| 11 | 431 | 67.5 | 28.5 | 6.0 | 218 | 1 |
| 12 | 522 | 60.6 | 28.3 | 6.3 | 226 | 1 |
| 13 | 628 | 62.2 | 29.8 | 6.1 | 222 | 1 |
| 14 | 136 | 68.8 | 28.0 | 6.1 | 222 | 0.6 |
| 15 | 227 | 66.5 | 28.0 | 6.0 | 218 | 0.6 |
| 16 | 338 | 68.0 | 28.2 | 6.5 | 235 | 0.6 |
| 17 | 454 | 69.4 | 28.8 | 6.7 | 241 | 0.6 |
| 18 | 539 | 67.6 | 28.0 | 6.5 | 235 | 0.6 |
| 19 | 630 | 69.2 | 27.7 | 6.7 | 241 | 0.6 |
| 20 | 535 | 66.7 | 27.2 | 9.0 | 309 | 1 |
| 21 | 559 | 66.4 | 27.0 | 12.0 | 381 | 1 |

Figure 6 shows characteristic curve for the oil flow in the system. The figure shows a parabolic relationship between the oil flow rate and pressure when oil is operating at an average temperature of 66.5 °C. Oil flow rate is strongly dependent on temperature, and is inversely proportional to viscosity. The higher the oil temperature, the lower is its viscosity and therefore the higher is the flow rate. In all test cases, the stainless steel plate is heated to a temperature ranging from 115 to around 630 °C. Thermocouples of type K are imbedded into nine of the fifteen drilled holes around the center of the plate. The temperature time history of

the thermocouples is recorded using a digital data acquisition system (Omega Chartscan-1400). At the beginning of each test case, the plate is placed on an electric plate heater (Omega Model No. WS-605), and after the desired steady--state temperature is reached, the plate is then transported to be repositioned on a rack in the oil chamber just above the nozzle manifold. The oil pump is then turned ON while the data acquisition system records the temperature on the hard disk drive of a portable computer. Figures 7 through 9 show the temperature time history of the plate (based on the area-weighted average of the 9 thermocouple readings) for cases 1 through 7 ($P_{oil}$ ~3 psi, $z$ = 1 cm), cases 8 through 13 ($P_{oil}$ ~6 psi, $z$ = 1 cm), and cases 14 through 19 ($P_{oil}$ ~6 psi, $z$ = 0.6 cm).

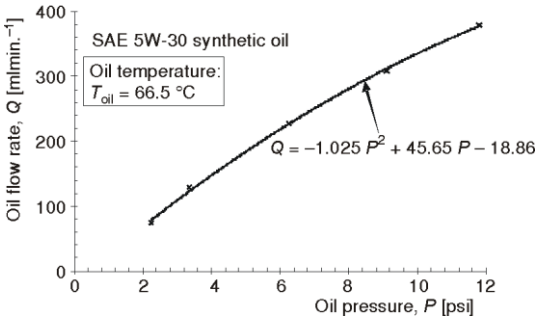


**Figure 6. Oil flow rate *vs.* operating pressure**

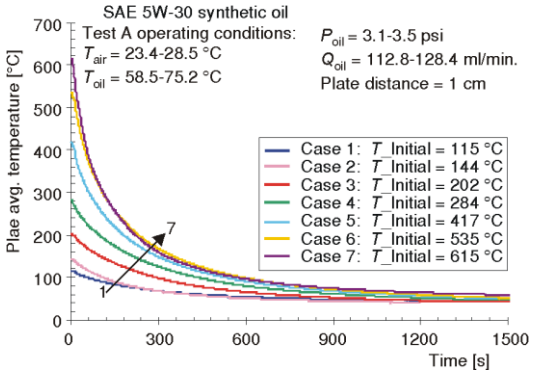


**Figure 7. Temperature time history for cases 1 through 7 ($P_{oil}$ ~ 3 psi, $z$ = 1 cm)**

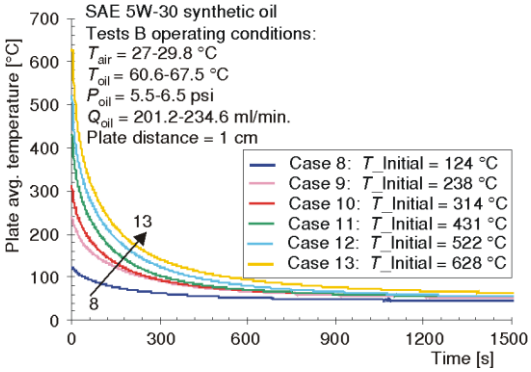


**Figure 8. Temperature time history for cases 8 through 13 ($P_{oil}$ ~ 6 psi, $z$ = 1 cm)**

The thickness of the plate was chosen to be thin enough so that lumped capacitance method to be valid in the evaluation of the oil heat transfer coefficient, and the inverse conduction method is not necessary. Since oil in general has a low heat transfer coefficient (much lower than that of water) the Biot number associated with oil quenching is less than 0.1 for the cases considered. Therefore, the heat transfer coefficient can be calculated from:

$$mc\frac{\mathrm{d}T}{\mathrm{d}t} = h_t A_s (T - T_\infty) \tag{8}$$

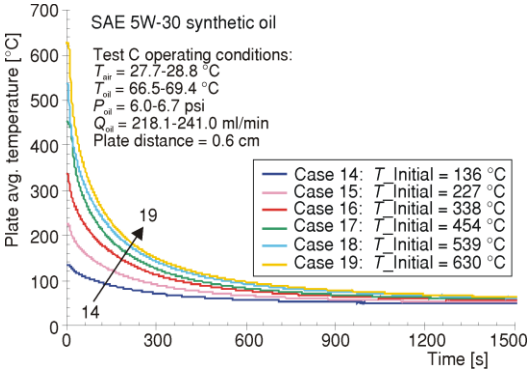


**Figure 9. Temperature time history for cases 14 through 19 ($P_{oil}$ ~ 6 psi, $z$ = 0.6 cm)**

The Biot number is defined as:

$$\mathrm{Bi} = \frac{h_\mathrm{t} L_\mathrm{c}}{k_\mathrm{s}} \tag{9}$$

where $L_\mathrm{c}$ is the characteristic length defined as the plate thickness, $L$. In the experimental setup, the plate bottom surface is exposed to oil, while the top surface (where thermocouples are installed) is covered by a layer of cement to secure the thermocouples in place. This cement layer acts as insulation on the top surface.

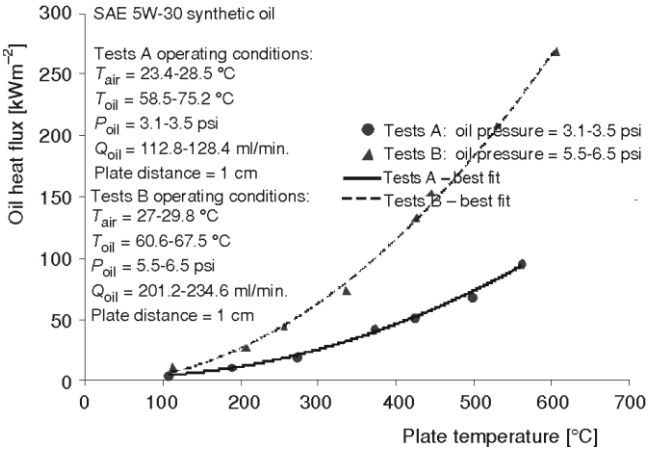


**Figure 10. Oil heat flux *vs.* plate temperature for various operating pressures ($z$ = 1 cm)**

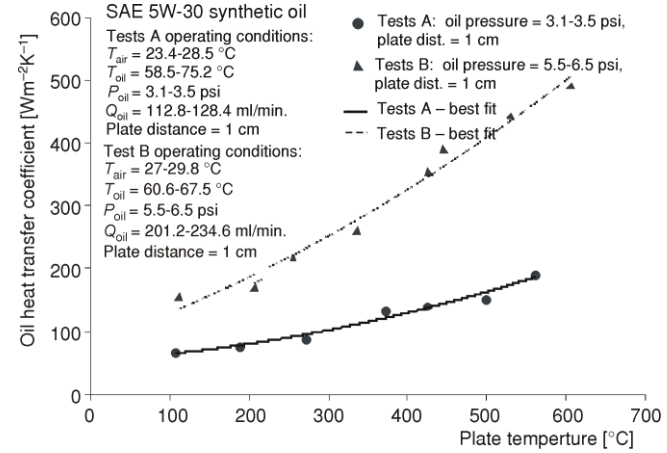


**Figure 11. Oil heat transfer coefficient *vs.* plate temperature for various operating pressures ($z$ = 1 cm)**

Radiation heat transfer at low temperatures (~100 °C) corresponds to about 5% of the total heat transfer, but this increases to about 19% for temperatures around 630 °C. Stainless steel material oxidizes at high temperatures, and the plate emissivity is approximated to be 0.8. The oil heat transfer cofficient is calculated by subtracting the effective radiation heat transfer, $h_\mathrm{r}$, from the total heat transfer coefficient, $h_\mathrm{t}$.

Figures 10 and 11 show the calculated oil heat flux and heat transfer coefficient for various operating pressures and surface temperatures. The results are presented for the configuration where the oil jet distance is 1 cm. The results show the oil heat flux keeps increasing for increasing plate temperature. The figure also shows the oil heat flux and heat transfer coefficient to be strongly dependent on the jet pressure. The increase in the operating pressure from about 3 to 6 psi results in an increase in heat flux and heat transfer coefficient by a factor close to 2.5 at high temperatures. Figures 12 and 13 show the effect of the oil jet distance on both the heat flux and heat transfer coefficient. Two jet distances are considered: 1 and 0.6 cm, where the operating oil pressure ranges from 5.5 to 6.7 psi. For both distances, the oil jet is able to

reach the target surface. As the distance decreases from 1 to 0.6 cm, the oil heat flux and heat transfer coefficient increases by about 20% at high temperatures. The effect of oil pressure on the heat transfer is much stronger than the effect of oil jet distance. The increase in oil pressure results in the jet having an impaction force (or jet momentum) higher than the impaction force resulting from the decrease in surface distance. The higher the impaction force (or jet momentum), the more the oil will spread at the surface during impaction, and the higher will be the heat transfer. Figure 14 shows the effect of pressure on the heat transfer coefficient for the jet distance of 1 cm. As the pressure increases from 3 to 12 psi, the oil heat transfer coefficient increases from 141 to 679 W/m$^2$K, an increase of 480% corresponding to a quadruple increase in pressure.

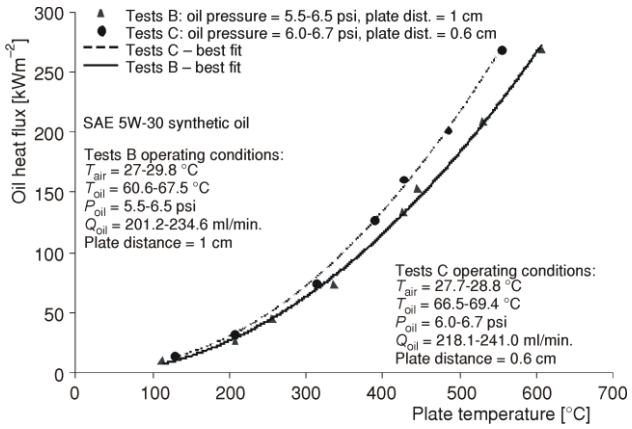


**Figure 12. Effect of oil jet distance on heat flux ($z$ = 1 cm *vs*. 0.6 cm)**

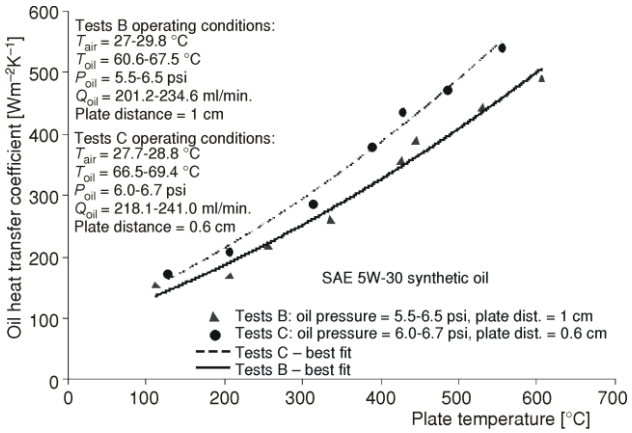


**Figure 13. Effect of oil jet distance on heat transfer coefficient ($z$ = 1 cm *vs*. 0.6 cm)**

Figure 15 shows a summary of results compiled from the various tests. The figure shows the effect of Reynolds number on the heat transfer coefficient while allowing the temperature to slightly vary within a narrow range. Four separate groups based on narrow temperature ranges are shown. The oil heat transfer coefficient is presented as function of the oil jet Reynolds number defined as:

$$\mathrm{Re}_\mathrm{D} = \frac{\rho_\mathrm{oil} V_\mathrm{n} D}{\mu_\mathrm{oil}} \tag{10}$$

where $D$ is the diameter of the nozzle exit (~1 mm). The oil heat transfer coefficient substantially increases with the increase in surface temperature and the flow Reynolds number. The effect from Reynolds number on heat transfer is due to the fact that the higher the Reynolds number, the higher will be the jet momentum and the more the oil film will spread at the surface during impaction leading to a larger oil surface to metal surface contact area. If the oil heat transfer coefficient is plotted against a non-dimensional parameter defined to be a function of jet flow Reynolds number ($\mathrm{Re}_\mathrm{D}$) and normalized temperature $(T_\mathrm{s} - T_\infty)/T_\infty$, then a

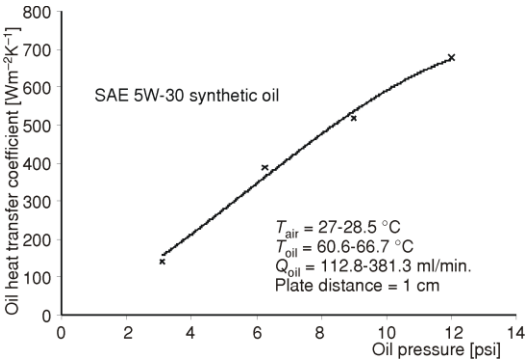


**Figure 14. Effect of oil pressure on heat transfer coefficient ($z$ = 1 cm)**

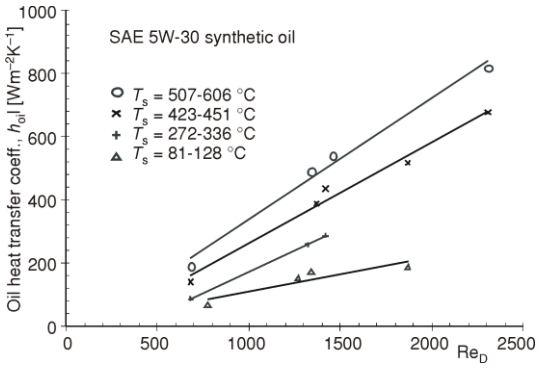


**Figure 15. Oil heat transfer coefficient *vs.* Reynolds number**

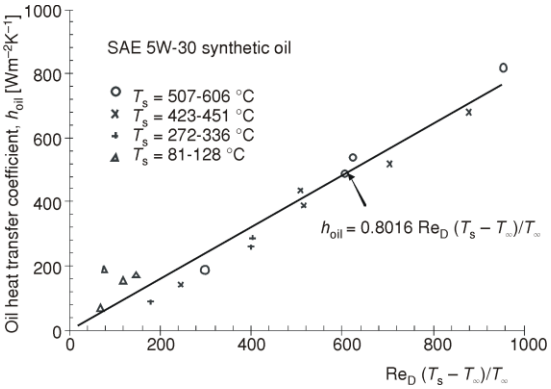


**Figure 16. Oil heat transfer coefficient *vs.* $Re_D(T_s - T_\infty)/T_\infty$**

clear relationship can be seen to exist between the oil heat transfer coefficient and the temperature-weighted Reynolds number as shown in fig. 16.

An empirical correlation can be obtained for the oil heat transfer coefficient *vs.* the jet Reynolds number, the surface and film temperature:

$$h_{\text{oil}} = 0.8016\,\text{Re}_{\text{D}}\,\frac{T_{\text{s}} - T_\infty}{T_\infty} \tag{11}$$

where $T_\infty$ is considered to be the ambient average temperature (average temperature between the oil and ambient air).

## Conclusions

Experimental studies are conducted for the oil quenching of a downward-facing stainless steel plate using a single oil jet. The plate is heated to temperatures ranging from 115 to 630 °C. Several tests are performed to investigate the effect of the plate surface temperature, oil pressure and flow rate, and nozzle-to-plate distance on the heat transfer coefficient. Test results show the heat transfer coefficient (and heat flux) to substantially increase with the increase in the oil operating pressure (or flow rate). This is because as the pressure or flow rate increases, the jet momentum also increases, and therefore, overcoming the effect of the gravitational and drag forces. As a result, the oil film spreads more during impaction to enhance the cooling effectiveness on the surface.

Test results also show that the oil heat transfer coefficient and heat flux keep increasing for increasing plate temperature. Comparing the boiling curves for oil to water, the boiling curve for oil shifts to a higher temperature range where the peak in the heat transfer can be expected to occur at a temperature much higher than that required for water. Also,

nozzle-to-plate distance has an effect on the heat transfer. However, the effect from increasing the oil pressure on the heat transfer is much stronger than the effect of reducing the nozzle-to--plate distance.

The oil heat transfer coefficient is shown to be a function of the oil jet Reynolds number, and the ambient (oil and air) average temperature. A strong relationship is shown to exist between the oil heat transfer coefficient and the temperature-weighted Reynolds number.

## Nomenclature

$A_s$ – plate surface area, [m$^2$]
Bi – Biot number, [–]
$c$ – stainless steel specific heat constant, [Jkg$^{-1}$K$^{-1}$]
$D$ – oil jet nozzle exit diameter, [m]
g – gravitational acceleration, [ms$^{-2}$]
$L$ – spindle length, [m]
$L_c$ – plate characteristic length, [m]
$m$ – stainless steel plate mass, [kg]
$n$ – power law index
$R_c$ – container radius, [m]
$\mathrm{Re}_D$ – Reynolds number for oil jet with diameter $D$
$R_s$ – spindle radius, [m]
$T$ – temperature, [°C]
$T_m$ – motor torque, [Nm]
$T_s$ – plate surface temperature, [°C]
$T_\infty$ – ambient average temperature, [°C]
$h_{oil}$ – oil heat transfer coefficient, [Wm$^{-2}$K$^{-1}$]
$h_t$ – total heat transfer coefficient, [Wm$^{-2}$K$^{-1}$]
$K$ – consistency coefficient
$k_s$ – thermal conductivity of stainless steel, [Wm$^{-1}$K$^{-1}$]
$t$ – time [s]
$V_n$ – oil velocity at the nozzle exit, [ms$^{-1}$]
$V_s$ – oil jet surface velocity, [ms$^{-1}$]
$z$ – nozzle-to-plate distance, [m]

*Greek symbols*

$\dot{\gamma}$ – shear rate, [s$^{-1}$]
$\mu$ – dynamic viscosity, [Nsm$^{-2}$]
$\mu_{oil}$ – oil dynamic viscosity, [Nsm$^{-2}$]
$\rho_{oil}$ – oil density, [kgm$^{-3}$]
$\tau$ – oil shear stress, [Nm$^{-2}$]
$\omega$ – spindle angular velocity, [rad·s$^{-1}$]

## References

[1] Incropera, F. P., DeWitt, D. P., Fundamentals of Heat and Mass Transfer, John Wiley & Sons, New York, USA, 1985
[2] Pais, M. R., Chow, L. C., Multiple Jet Impingement Cooling, *Journal of Thermophysics and Heat Transfer*, *7* (1993), 3, pp. 435-440
[3] Lamvik, M., Iden, B. A., Heat Transfer Coefficient by Water Jets Impinging on a Hot Surface, *Proceedings* (Eds. V. Grigul *et al.*) 7th International Heat Transfer Conference, Munich, FR Germany, 1982, Vol. 3, FC64, pp. 369-375
[4] Ishigai, S., Nakanishi, A., Ochi, T., Boiling Heat Transfer for a Plane Water Jet Impinging on a Hot Surface, 6th International Heat Transfer Conference, Toronto, Canada, 1978, pp. 601-610
[5] Issa, R., Yao, S. C., A Numerical Model for Spray-Wall Impactions and Heat Transfer at Atmospheric Conditions, *Journal of Thermophysics and Heat Transfer*, *19* (2005), 4, pp. 441-447
[6] Issa, R. J., Optimal Spray Characteristics in the Air-Assisted Water Spray Cooling of a Downward-Facing Heated Surface, 24th ASM International Heat Treating Society Conference, Detroit, Mich., USA, 2007
[7] Chen, N., *et al*., Enhancing Mechanical Properties and Avoiding Cracks by Simulation of Quenching Connecting Rods, *Materials Letters*, *61* (2007), 14-15, pp. 3021-3024
[8] Abou-Ziyan, H. Z., Heat Transfer Characteristics of Some Oils Used for Engine Cooling, *Energy Conversion and Management*, *45* (2004), 15-16, pp. 2553-2569
[9] Prabhu, K. N., Fernandes, P., Effect of Surface Roughness on Metal/Quenchant Interfacial Heat Transfer and Evolution of Microstructure, *Materials and Design*, *28* (2007), 2, pp. 544-550
[10] Fernandes, P., Prabhu, K. N., Effect of Section Size and Agitation on Heat Transfer During Quenching of AISI 1040 Steel, *Journal of Materials Processing Technology*, *183* (2007), 1, pp. 1-5
[11] De Paepe, M., Bogaert, W., Mertens, D., Cooling of Oil Injected Screw Compressors by Oil Atomization, *Applied Thermal Engineering*, *25* (2005), 17-18, pp. 2764-2779

[12] Ma, C. F., *et al*., Local Characteristics of Impingement Heat Transfer with Oblique Round Free-Surface Jets of Large Prandtl Number Liquid, *Int. J. Heat Mass Transfer*, *40* (1997), 10, pp. 2249-2259
[13] Akbarpour, M. R., High Temperature Mechanical Properties of Triple Phase Steels, *Materials Letters*, *61* (2007), 4-5, pp. 1023-1026
[14] Zhukauskas, A. A., Ambrazyavichyus, A. B., Heat Transfer of a Plate in a Liquid Flow, *Int. J. Heat Mass Transfer*, *3* (1961), 4, pp. 305-309
[15] Macosko, C. W., Rheology Principles, Measurement, and Applications, John Wiley and Sons, New York, USA, 1994

Paper submitted: April 6, 2009
Paper revised: April 5, 2010
Paper accepted: January 6, 2011